# Update on the Offline Analysis Framework for AugerPrime and integration of the AugerPrime Radio Detector reconstruction

*Marvin* Gottowik[1] for the Pierre Auger Collaboration[2,*]

[1]Karlsruher Institut für Technologie, Institut für Astroteilchenphysik, Karlsruhe, Germany
[2]Observatorio Pierre Auger, Av. San Martín Norte 304, 5613 Malargüe, Argentina

**Abstract.** The Offline Framework serves as a comprehensive tool for the reconstruction of measured data and simulated air showers for the Pierre Auger Observatory. Originally developed for the Surface and Fluorescence Detectors, new detectors such as the Auger Engineering Radio Array have already been successfully integrated. The development and installation of the AugerPrime upgrade required incorporating new detector types and updating existing detector descriptions. This integration was facilitated by the modular structure of Offline, which strictly separates detector descriptions, data structures, and processing modules. We will discuss the general structure of the Offline Framework and explain the design decisions that provided its flexibility. Specifically, we will describe the reconstruction of data from the AugerPrime Radio Detector within Offline. This includes the signal reconstruction for each station, the directional reconstruction based on a spherical model of the signal arrival time at all stations, and the energy and distance to $X_{\mathrm{max}}$ reconstruction from a fit of the lateral signal distribution. Additionally, we will outline anticipated improvements in the reconstruction process, such as an absolute calibration based on the galactic radio emission and an advanced suppression technique for narrow-band RFI pulses.

## 1 The Pierre Auger Observatory

The Pierre Auger Observatory [1], located in the Mendoza province of Argentina, is the world's largest facility for studying ultra-high-energy cosmic rays. It was designed with a hybrid detection system consisting of two complementary techniques: a Surface Detector (SD) array of 1600 water-Cherenkov detector stations [2] spread over an area of 3000 km$^2$ and a Fluorescence Detector (FD) with 24 telescopes at four sites surrounding the array [3]. The SD detects the secondary particles of extensive air showers, while the FD observes the faint fluorescence light emitted as the showers develop in the atmosphere, allowing a precise reconstruction of the properties of cosmic rays.

Over the years, the observatory has been expanded with specialized extensions to enhance its capabilities. Three High Elevation Auger Telescopes (HEAT) were added to improve sensitivity to low-energy cosmic rays by observing showers at higher elevations [4]. The Underground Muon Detectors (UMD) were deployed to directly measure muons in air showers [5],

*e-mail: spokespersons@auger.org, full author list: https://www.auger.org/archive/authors_2024_09.html

critical for probing hadronic interactions. The Auger Engineering Radio Array (AERA) was installed to explore radio emissions from cosmic-ray-induced air showers [6], which offers a complementary detection method.

The current upgrade, AugerPrime [7], is designed to enhance the ability to differentiate cosmic-ray primaries on an event-by-event basis. The key components of AugerPrime include the addition of Scintillator Surface Detectors (SSD) atop the original SD tanks for an improved particle-type separation, small photomultiplier tubes (PMTs) in the SD stations for an enhanced dynamic range, and a Radio Detector (RD) to further expand radio detection capabilities [8]. These upgrades will enable the observatory to address fundamental questions about cosmic rays and their sources with unprecedented precision.

## 2 The $\overline{\text{Off}}\underline{\text{line}}$ Analysis Framework

The $\overline{\text{Off}}\underline{\text{line}}$ Analysis Framework [9] of the Pierre Auger Observatory is a flexible, modular software framework designed to facilitate the reconstruction, simulation, and analysis of data from the observatory's diverse detector systems. Its structure is built around a central event data model enabling seamless integration of data from all detector systems. The framework includes a library of modular algorithms for individual tasks during event reconstruction, calibration, and high-quality selection, as well as tools for detector simulation. By supporting a wide range of input and output formats, it ensures compatibility with real observational data and Monte Carlo simulations. Its purpose is to provide a standardized and efficient platform for analyzing the complex datasets produced by the observatory.

Thanks to the modular design, $\overline{\text{Off}}\underline{\text{line}}$ has previously been adapted to integrate various detector types, such as AERA, as detailed in [10]. Recently, the framework has been extended to incorporate the new AugerPrime detectors. The necessary modifications for this integration are described, for instance, in [11]. In this proceeding, we focus specifically on the integration of the RD event reconstruction into $\overline{\text{Off}}\underline{\text{line}}$. We benefited from the experience made with AERA and were able to reuse functionality included to accommodate AERA for the RD reconstruction. We will discuss our current station signal reconstruction, as well as directional reconstruction and lateral signal fitting for the entire radio event. The following description of the reconstruction performance is largely based on reference [12]. The performance of the reconstruction is validated on a large set of CoREAS [13] simulations using p, He, Ni, and Fe as primary particles with isotropic arrival directions for zenith angles within 65° to 85° and primary energies between $10^{18.4}$ eV and $10^{20.1}$ eV. They are reconstructed with $\overline{\text{Off}}\underline{\text{line}}$ including a realistic detector simulation and the addition of measured noise. In addition, we will outline further anticipated improvements in the reconstruction pipeline.

## 3 Station signal reconstruction

To extract the electric field pulse from the measured voltage trace of a detector station, one has to unfold the antenna response, which is described via the vector effective length that depends on the frequency and the shower direction. For a given shower direction, usually given by the SD reconstruction, this equation is solved in spherical coordinates with two orthogonal polarized antennas, as the electric field has no component in the direction of propagation [14]. The pulse position, i.e. the signal time, and the pulse amplitude are determined by the Hilbert envelope of the electric field trace as the bandpass-filtered trace itself can have a zero-crossing at the position of the pulse maximum.

The energy fluence measured at a given station, i.e. the energy deposit per unit area, is currently estimated using the "noise-subtraction method". It is given by the time integral of

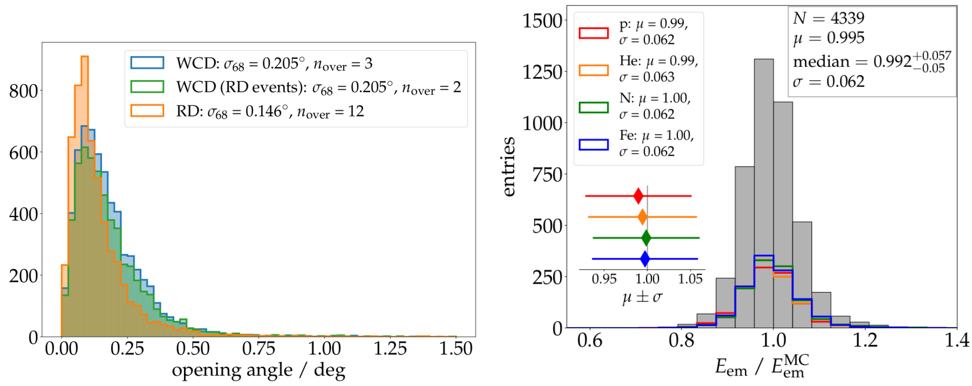


**Figure 1.** Opening-angle distributions for the RD- and WCD-reconstructed shower axes w.r.t. the MC shower axis (left). Histogram of reconstructed and MC-true electromagnetic energy for the set of all high-quality events and for each primary individually (right). Figures from [12].

the absolute value of the Poynting vector over the signal window centered at the signal time and subtracting a noise contribution determined in a time window where no signal contribution is expected [15]. This method works very well for strong signals but is biased for stations with a low signal-to-noise ratio. Therefore, we are currently investigating an improved signal estimation in the presence of noise based on a robust and rigorous statistical background [16].

## 4 Directional reconstruction

The incoming direction of the air shower can be reconstructed from the arrival time of the radio pulse measured by individual radio stations using an assumption on the shape of the radio wavefront. For inclined air showers with a zenith angle above 60°, we use a spherical wavefront model as the emission region is far away from the observer on the ground. Hence, we can assume a point source whose position is described in spherical coordinates by three fit parameters: the zenith and azimuth angles and the distance from the SD core position.

The spherical wavefront fit yields an accurate reconstruction of the incoming direction. For a large set of simulations, we calculate the opening angle between the reconstructed and the MC-true shower direction, cf. Fig. 1 (left). We obtain an angular resolution, defined as the 68%-quantile of this distribution, of 0.146°. In principle, the distance from the source location is an estimator of the distance to $X_{max}$. However, as it turns out, the reconstruction is, in general, not accurate enough to be useful.

## 5 Electromagnetic energy reconstruction

The lateral distribution of the signal strength is described using a model specifically developed for inclined air showers [17]. The model describes the highly asymmetric signal distribution of the radio emission in the $\vec{v} \times \vec{B}$ polarization depending on shower core position, geomagnetic radiation energy, and the distance to $X_{max}$. The geomagnetic radiation energy is used to estimate the electromagnetic energy of the air shower, $E_{EM}$. The performance of the reconstruction is evaluated for a subset of simulated high-quality events. A histogram of the bias is shown in Fig. 1 (right). We find a bias-free reconstruction with a resolution of 6.2 %. No notable primary-dependent reconstruction bias was found.

## 6 Anticipated improvements

A relative measurement of the directional response of the antenna is performed by a drone calibration. The first results are in overall agreement with the response pattern obtained from simulations [18]. An absolute calibration can be performed using the continuously monitored sidereal modulation of the diffuse Galactic radio emission. Preliminary results obtained for AERA yield calibration constants that are consistent with unity within uncertainties [19]. This indicates a good agreement with the original calibration process, which included laboratory measurements of the analog chain, and simulations to ascertain the directional response of the antennas. Similar analyses are already being performed for the RD [20].

We are also investigating an improved method for the removal of strong narrowband radio frequency interference (RFI). Narrowband RFI occurs frequently in measurements due to technological radio noise or the AERA beacon [21]. The improved method finds the frequency and corresponding phase with the highest amplitude using a discrete-time Fourier transform and subtracts the corresponding sine wave in the time domain. This procedure is repeated iteratively as long as a significant reduction of trace RMS is obtained or until a maximal number of frequencies is removed. This method substantially reduces the RMS of the trace, allowing for improved reconstruction of low-signal stations and an increased number of events at lower energies. The exact impact of this RFI removal method has yet to be quantified.

## 7 Conclusions

The modular design of $\overline{\text{Off}}\underline{\text{line}}$ has proven to be highly effective in adapting to the evolving needs of the Pierre Auger Observatory. This flexibility has enabled the successful integration of new detector types introduced by the AugerPrime upgrade, including the RD, into the existing framework. The simulation and reconstruction processes for the RD are now fully incorporated, leveraging previous experience with the Auger Engineering Radio Array. These developments have facilitated advanced reconstruction methods, achieving a high accuracy in the data analysis.

## References

[1] A. Aab *et al.*, Nucl. Instrum. Meth. A **798** (2015) 172–213.
[2] I. Allekotte *et al.*, Nucl. Instrum. Meth. A **586** (2008) 409–420.
[3] J. Abraham *et al.*, Nucl. Instrum. Meth. A **620** (2010) 227–251.
[4] C. Meurer and N. Scharf for the Pierre Auger Collaboration, Astrophys. Space Sci. Trans. **7** (2011) 183–186.
[5] J. Jesus for the Pierre Auger Collaboration, PoS(ICRC2023)267.
[6] E. M. Holt for the Pierre Auger Collaboration, PoS(ICRC2017)492.
[7] A. Aab *et al.*, The Pierre Auger Observatory Upgrade - Preliminary Design Report, 2016, arXiv:1604.03637.
[8] J. Pawlowsky for the Pierre Auger Collaboration, PoS(ICRC2023)344.
[9] S. Argirò *et al.*, Nucl. Instrum. Meth. A **580** (2007) 1485–1496.
[10] P. Abreu *et al.*, Nucl. Instrum. Meth. A **635** (2011) 92–102.
[11] E. Santos for the Pierre Auger Collaboration, PoS(ICRC2023)248.
[12] F. Schlüter, PhD thesis, Karlsruhe Institute of Technology (KIT), 2022, doi: 10.5445/IR/1000149113.
[13] T. Huege, M. Ludwig, and C. W. James, AIP Conf. Proc. **1535** (2013) 128.
[14] P. Abreu *et al.*, JINST **7** (2012) P10011.
[15] A. Aab *et al.*, Phys. Rev. D **93** (2016) 122005.
[16] S. Martinelli *et al.*, submitted to Astroparticle Physics, arXiv:2407.18654.
[17] F. Schlüter and T. Huege, JCAP, **01** (2023) 8.
[18] A. Reuzki for the Pierre Auger Collaboration, PoS(ARENA2024)029.
[19] D. C dos Santos for the Pierre Auger Collaboration, PoS(ARENA2024)030.
[20] T. Fodran for the Pierre Auger Collaboration, PoS(ARENA2022)043.
[21] A. Aab *et al.*, JINST **11** (2016) 1018.